Available online at www.sciencedirect.com
ScienceDirect
International Journal of Thermal Sciences 46 (2007) 444–457
International Journal of Thermal Sciences
www.elsevier.com/locate/ijts

Transient heating of a semitransparent spherical body ☆

Sergei S. Sazhin [a,*], Pavel A. Krutitskii [b], Serguei B. Martynov [a], David Mason [a], Morgan R. Heikal [a], Elena M. Sazhina [a]

[a] *School of Engineering, Faculty of Science and Engineering, University of Brighton, Cockcroft Building, Brighton BN2 4GJ, UK*
[b] *Faculty of Physics, Moscow State University, Vorobyovy gory, Moscow 119899, Russia*

Received 22 December 2005; received in revised form 3 July 2006; accepted 3 July 2006

Available online 12 September 2006

Abstract

The problem of transient heating of a semitransparent spherical body immersed in a stationary hot gas is investigated, taking into account the effect of thermal radiation. The size of the domain occupied by the gas is assumed to be finite, and the outer boundary of this domain is kept at constant temperature. The initial radial distribution of temperature in the body is taken into account. A modification of Newton's law for body heating is introduced via a correction to either the gas temperature or convection heat transfer coefficient. Explicit expressions for these corrections are obtained for the case of homogeneous initial distribution of temperature and radiation absorption inside the body, and constant radiation temperature. For large Fourier numbers *Fo*, the correction to gas temperature is expected to be of limited practical importance, as both this correction and the difference between the initial gas temperature and the body surface temperature approach zero (heat transferred from gas to the body becomes negligible). The results are analysed using values of parameters relevant to diesel engines. The values of the corrections to the convection heat transfer coefficient vary from about 0.1 (large domain occupied by gas and $Fo = 500$) to 2.8 at $Fo = 0.1$. This means that ignoring these corrections is expected to lead to unacceptably large errors in computations. The total time for body heating is shown to be more than an order of magnitude longer when compared to the heating of this body in a perfectly stirred gas. The effect of thermal radiation on droplet heating is accounted for via the additional corrections of gas temperature or the convection heat transfer coefficient. It is shown that the effects of radiation on the surface heat flux are small for small *Fo*, but become dominant for large *Fo* ($Fo > 50$).

Keywords: Conduction; Thermal radiation; Semi-transparency; Droplets

1. Introduction

The conventional approach to modeling the heating of a spherical body immersed in a hot gas is based on the application of Newton's law, according to which the heat flux from gas to droplets is estimated as [1]:

$$\dot{q} = h(T_{g0} - T_s) \tag{1}$$

where T_s is the temperature of the surface of the body, T_{g0} is the ambient gas temperature, $h = Nu\,k_g/2R_b$, Nu is the Nusselt number, k_g is the gas thermal conductivity, R_b is the radius of the body. For quasi-stationary processes (the boundary layer around a body has enough time to develop) when $Re = 0$ and in the absence of natural convection, it is known that $Nu = 2$ and $h = k_g/R_b$ [1]. The transient heating of a sphere, kept at constant temperature and immersed in a hot gas, was considered in several papers including [2–4]. Ignoring the contribution of droplet relative velocity and the effects of natural convection, it was shown that Eq. (1) with $Nu = 2$ can still be used if we replace gas thermal conductivity by the time-dependent effective thermal conductivity.

A more general problem of heating of a spherical body, based on a coupled solution of the heat conduction equation in the body and the gas was solved in [5]. The solution was based on the Laplace transform and the gas medium was assumed to be infinite. The initial body and gas temperatures were assumed to be constant. Although the temperature distribution

☆ Authors are grateful to EPSRC (Grant GR/R82920/01) and European Regional Development Fund (Franco–British IIIa Programme 2000–2006; Project Ref. 162/025/247) for financial support of this project.
* Corresponding author.
E-mail address: s.sazhin@bton.ac.uk (S.S. Sazhin).

1290-0729/$ – see front matter
doi:10.1016/j.ijthermalsci.2006.07.007

Nomenclature

a	coefficient introduced in Eq. (4)	m^{-b}
A	function defined by Eq. (A.11)	
$a_{b,g}$	coefficients introduced in Eq. (8)	$\sqrt{s}\,m^{-1}$
A_n	coefficients introduced in Eqs. (14) and (15)	$m^3\,K\,W^{-1}$
$a_{0,1,2}$	coefficient used in the estimate of a	
b	coefficients introduced in Eq. (4) or following Eq. (A.14)	$J\,m^{-3}\,K^{-1}$
B	function defined by Eq. (A.11)	
$b_{0,1,2}$	coefficient used in the estimate of b in Eq. (4)	
c	specific heat capacity	$J\,kg^{-1}\,K^{-1}$
Fo	Fourier number	
h	convective heat transfer coefficient	$W\,m^{-2}\,K^{-1}$
k	thermal conductivity	$W\,m^{-1}\,K^{-1}$
Nu	Nusselt number	
P	radiation source in Eq. (2)	$K\,s^{-1}$
$p_n(t)$	functions introduced in Eq. (7)	$K\,m\,s^{-1}$
$\dot{q}$	heat flux	$W\,m^{-2}$
R	distance from the center	m
$\widetilde{R}_{(g)}$	$R_{(g)}/R_b$	
$\widetilde{R}_n$	$\pi n R/R_b$	
t	time	s
T	temperature	K
$\widetilde{T}$	$(T_{g0}-T)/(T_{g0}-T_{b0})$	
u	$(T-T_{g0})R$	
v_n	eigenfunctions found from Eq. (8)	
$\|v_n\|^2$	norm of v_n with weight b	$J\,m^{-2}\,K^{-1}$

Greek symbols

ΔT_c, ΔT_r	functions introduced in Eqs. (14) and (15)	K
$\Delta\widetilde{T}_c$	$-\Delta T_c/(T_{g0}-T_{b0})$	
ε	$\sqrt{k_g c_{pg}\rho_g/(k_b c_b \rho_b)}$	
ζ	$\Delta T_c/\Delta T_r$	
$\Theta_n(t)$	function defined by Eq. (A.21)	K m
θ_R	radiation temperature	K
κ	thermal diffusivity	$m^2\,s^{-1}$
λ_n	eigenvalues found from Eq. (9)	$s^{-0.5}$
$\tilde{\lambda}_n$	$\lambda_n a_b R_b/\pi$	
ξ	$(T_{g0}-T_{s(r)})/(T_{g0}-T_{s(c)})$	
ρ	density	$kg\,m^{-3}$
Φ	function introduced in Eq. (18)	
χ	parameter defined by Eq. (17)	

Subscripts

b	body
eff	effective
ext	external
g	gas
s	surface
0	initial

in the whole domain and the heat flux at the body boundary were calculated, no formal links with the Newton's law were investigated. Also, it remained unclear how the results could be used in computational fluid dynamics (CFD) codes, where the areas occupied by gas are limited by cell sizes, and how the non-constant initial distribution of temperature inside the body can be taken into account. The effects of thermal radiation were ignored.

Özişik [6] considered a rather general problem of heat transfer through N spherical layers. The author looked for separate solutions in each layer and then these solutions were matched by the conditions of continuity of temperatures and their derivatives. These conditions led to two systems of equations to find the relevant eigenfunctions and eigenvalues. These systems of equations, however, were not actually solved and thus the solution was not presented in an explicit form.

Numerical simulations of cooling and heating of spherical bodies with a view to various engineering applications have been reported in a number of papers, including [7,8].

The objective of this paper is to develop a general analytical model that describes the process of heating a spherical body immersed in a hot gas, taking into account the variations of body surface temperature (coupled solution), non-uniform initial distribution of temperature in the body, the effects of radiation, and the finite size of the domain occupied by the gas. The contribution of the flow around the body is ignored, but a direct link with the Newton's law is established. As in [6] our solution is based on the separation of variables and finding the relevant eigenfunctions and eigenvalues. In contrast to [6], however, we look for a solution in the whole domain (not in each layer separately) and finally obtain this solution in an explicit form. The boundary conditions are different from those used in [6]. The prediction of the model is compared with the prediction of Cooper's [5] solution.

The model is expected to have a wide range of potential engineering, environmental and medical applications, including heating of UO_2 particles (the problem considered in [5]), aerosols, droplets etc [9–13]. A number of simplifications of the model will be made in order to capture the main features of transient heating of a spherical body. These include decoupling of the heat transfer equation from the mass transfer equation in the gas phase, ignoring chemical reactions in the gas phase and interaction between bodies. Despite the above mentioned simplifications, the effect of the model will be illustrated for the values of parameters typical for diesel engines [14–17]. In this case we will be able to illustrate the trends of the processes taking into account the effects almost universally ignored in the previous studies, rather than suggest a comprehensive model of the phenomenon. The ways in which the developed model can be implemented into computational fluid dynamics codes will not be investigated (cf. analyses for fixed convection heat transfer coefficient reported in [18–22]).

The basic equations and approximations of the model are presented and discussed in Section 2. In Section 3 the analytical

solution is presented and discussed. The analysis of the solution for parameters typical for diesel engines is presented in Section 4. The main conclusions of the paper are summarized in Section 5.

2. Basic equations and approximations

Let us assume that a spherical body of radius R_b and initial temperature $T_{b0}(R)$ is immersed in the center of a homogeneous gaseous sphere of radius R_g at temperature T_{g0}. The outer surface temperature of the gaseous sphere remains constant and equal to T_{g0}. R_g is assumed to be greater than R_b, and finite. The variation of the temperatures in the gas-body domain is described by the heat conduction equation in the form [23,24]:

$$\frac{\partial T}{\partial t} = \kappa\left(\frac{\partial^2 T}{\partial R^2} + \frac{2}{R}\frac{\partial T}{\partial R}\right) + P(t,R) \tag{2}$$

where

$$\kappa = \begin{cases} \kappa_b = k_b/(c_b\rho_b) & \text{when } R \leqslant R_b \\ \kappa_g = k_g/(c_{pg}\rho_g) & \text{when } R_b < R \leqslant R_g \end{cases} \tag{3}$$

$\kappa_{b(g)}$ is the body (gas) thermal diffusivity, $k_{b(g)}$ is the body (gas) thermal conductivity, $c_{b(pg)}$ is the body (gas) specific heat capacity, $\rho_{b(g)}$ is the body (gas) density, R is the distance from the center of the sphere, t is time, $T(R_g) = T_{g0} = \text{const}$.

The radiation term is assumed zero outside the body: $P(t,R) = 0$ when $R_b < R \leqslant R_g$. $P(t,R)$ is discontinuous at $R = R_b$ in the general case. This assumption effectively means that we ignore the absorption of thermal radiation in the gas, and assume that the gas is optically thin [25]. The values of $P(t,R)$ for a specific semi-transparent substance could be calculated using the well-known Mie theory [26–29], but this would have been of limited practical importance. An approximate model describing the absorption of thermal radiation in symmetrically illuminated diesel fuel droplets was developed in [30]. It was further generalised in [28,29] for the case of symmetric and asymmetric illumination of droplets. In [31,32], on the other hand, a simplified model of thermal radiation absorption in diesel fuel droplets was developed, in which only the total amount of radiation absorbed in them was taken into account. In this case we can formally assume that thermal radiation is absorbed in them homogeneously. An approximate expression for $P(t,R)$ was derived in the form [18]:

$$P(R) = 3a\sigma R_b^{b-1}\theta_R^4/c_b\rho_b \tag{4}$$

where θ_R is the radiation temperature,

$$a = a_0 + a_1\theta_R/10^3 + a_2\left(\theta_R/10^3\right)^2$$

$$b = b_0 + b_1\theta_R/10^3 + b_2\left(\theta_R/10^3\right)^2$$

θ_R can be assumed equal to the external temperature in the case of an optically thin gas in the whole domain. In the case when gas is optically thin in the vicinity of the body $R_b < R < R_g$ only, we can assume that $\theta_R = T_g(R_g)$. In both cases our assumption that the absorption of thermal radiation in the gas is small compared with the absorption of thermal radiation in the body is valid. The radiative losses from the body are ignored, which is justified when the body temperature is well below θ_R. These assumptions are usually justified in engineering applications. In the following analysis the focus will be on optically thin gases in the whole domain when $\theta_R = T_{\text{ext}}$. In diesel engines this temperature can be associated with the temperature of remote flames, and can reach more than 2500 K [15]. The generalisation of the analysis to the case when $\theta_R = T_g(R_g)$ is straightforward.

As was shown in [18,33,34], even in the case of strong radiative heating of diesel fuel droplets, modeling of the detailed distribution of thermal radiation absorption in them, only slightly improves the accuracy of calculation when compared with the application of the simplified formula (4). This formula will be used in this paper although the solution will be presented for the general case $P(R,t)$. The expressions for the coefficients a and b for a typical automotive diesel fuel (low sulphur ESSO AF1313 diesel fuel) in the range of external temperatures 1000–3000 K, obtained in [32], will be used.

Eq. (2) needs to be solved subject to initial and boundary conditions:

$$T|_{t=0} = \begin{cases} T_{b0}(R) & \text{when } R \leqslant R_b \\ T_{g0} & \text{when } R_b < R \leqslant R_g \end{cases} \tag{5}$$

$$T|_{R=R_b^-} = T|_{R=R_b^+}$$

$$k_b\left.\frac{\partial T}{\partial R}\right|_{R=R_b^-} = k_g\left.\frac{\partial T}{\partial R}\right|_{R=R_b^+}$$

$$T|_{R=R_g} = T_{g0} \tag{6}$$

Note that for opaque bodies the effect of radiation could have been described via the modification of the boundary conditions (6) and not via introduction of the term $P(t,R)$ (see e.g. [35–37]). The analysis of this case is beyond the scope of this paper.

A number of simplifications of the model has been made in order to capture the main features of transient heating of a spherical body. These include decoupling of the heat transfer equation from the mass transfer equation in the gas phase, ignoring chemical reactions in the gas phase and interaction between bodies. Also, the ways in which the developed model can be implemented into computational fluid dynamics codes have not been investigated (cf. a similar analysis for fixed convection heat transfer coefficient reported in [18–20]).

3. Analytical solutions

The solution of Eq. (2) subject to initial and boundary conditions (5)–(6) in the limiting case of $R_g \to \infty$, $T_{b0} = \text{const}$ and in the absence of radiation was reported in [5]. We obtained an alternative form of this solution, based on the assumption that R_g is finite, T_{b0} depends on R and taking into account the contribution of thermal radiation (see Appendix A):

$$T(R,t) = T_{g0} + \frac{1}{R}\sum_{n=1}^{\infty}\left[\exp\left(-\lambda_n^2 t\right)\frac{1}{\|v_n\|^2} \times \int_0^{R_b}\left(-\left(T_{g0} - T_{b0}(R)\right)\right)Rv_n(R)c_b\rho_b\,\mathrm{d}R\right.$$

$$+\int_0^t \exp\bigl(-\lambda_n^2(t-\tau)\bigr)p_n(\tau)\,\mathrm{d}\tau\Bigg]v_n(R) \tag{7}$$

where

$$v_n(R)=\begin{cases}\frac{\sin(\lambda_n a_b R)}{\sin(\lambda_n a_b R_b)} & \text{when } R<R_b\\ \frac{\sin(\lambda_n a_g(R-R_g))}{\sin(\lambda_n a_g(R_b-R_g))} & \text{when } R_b\leqslant R\leqslant R_g\end{cases} \tag{8}$$

$$\|v_n\|^2=\frac{c_b\rho_b R_b}{2\sin^2(\lambda_n a_b R_b)}+\frac{c_{pg}\rho_g(R_g-R_b)}{2\sin^2(\lambda_n a_g(R_b-R_g))}-\frac{k_b-k_g}{2R_b\lambda_n^2}$$

$$p_n(t)=\frac{c_b\rho_b}{\|v_n\|^2}\int_0^{R_b} RP(t,R)v_n(R)\,\mathrm{d}R$$

A countable set of positive eigenvalues λ_n is found from the solution of the equation:

$$\sqrt{k_b c_b\rho_b}\cot(\lambda a_b R_b)-\sqrt{k_g c_{pg}\rho_g}\cot\bigl(\lambda a_g(R_b-R_g)\bigr)=\frac{k_b-k_g}{R_b\lambda} \tag{9}$$

These are arranged in ascending order $0<\lambda_1<\lambda_2<\cdots$. $a_b=\sqrt{\frac{c_b\rho_b}{k_b}}$, $a_g=\sqrt{\frac{c_{pg}\rho_g}{k_g}}$.

If T_{b0} does not depend on R then Eq. (7) can be simplified to

$$T(R,t)=T_{g0}+\frac{1}{R}\sum_{n=1}^{\infty}\Bigg[\exp\bigl(-\lambda_n^2 t\bigr)\frac{(T_{g0}-T_{b0})\sqrt{k_b c_b\rho_b}}{\lambda_n\|v_n\|^2}\times\left[R_b\cot(\lambda_n a_b R_b)-\frac{1}{\lambda_n a_b}\right]+\int_0^t\exp\bigl(-\lambda_n^2(t-\tau)\bigr)p_n(\tau)\,\mathrm{d}\tau\Bigg]v_n(R) \tag{10}$$

In what follows the focus will be on this form of the solution. This solution can be further simplified if we ignore the dependence of P on R and t. In this case with a view of Eq. (4) the expression for p_n can be rewritten in a more explicit form:

$$p_n=\frac{3a\sigma R_b^{b-1}\theta_R^4}{\|v_n\|^2\lambda_n^2 a_b^2}\bigl[1-\lambda_n a_b R_b\cot(\lambda_n a_b R_b)\bigr] \tag{11}$$

Remembering our assumption that the body is stationary we can estimate the heat flux arriving at the surface of the body:

$$\dot q=k_g\frac{\partial T}{\partial R}\bigg|_{R=R_b+0}=k_b\frac{\partial T}{\partial R}\bigg|_{R=R_b-0}=\frac{k_g}{R_b}\bigl[T_{\mathrm{eff}}-T(R_b,t)\bigr] \tag{12}$$

where

$$T_{\mathrm{eff}}=T_{g0}+\Delta T_c+\Delta T_r=T_{g0}+\Delta T_c(1+\zeta) \tag{13}$$

$$\Delta T_c=(T_{g0}-T_{b0})k_b a_b a_g\sum_{n=1}^{\infty}A_n\exp\bigl(-\lambda_n^2 t\bigr) \tag{14}$$

$$\Delta T_r=-\frac{3a\sigma R_b^{b-1}\theta_R^4 a_g}{a_b}\sum_{n=1}^{\infty}\frac{A_n}{\lambda_n^2}\bigl(1-\exp\bigl(-\lambda_n^2 t\bigr)\bigr) \tag{15}$$

$$A_n=\frac{1}{\|v_n\|^2}\left[R_b\cot(\lambda_n a_b R_b)-\frac{1}{\lambda_n a_b}\right]\cot\bigl(\lambda_n a_g(R_b-R_g)\bigr)$$

$$\zeta=\Delta T_r/\Delta T_c$$

Eq. (12) describes Newton's law for a stationary body with $h=k_g/R_b$, in which T_{g0} is replaced by T_{eff}. ΔT_c and ΔT_r describe the required corrections to T_{g0} due to the effects of transient heat conduction and radiation, respectively. Note that the values of ΔT_c are expected to be maximal at $t\to 0$, when $\Delta T_r\to 0$. The values of $|\Delta T_r|$ are expected to be maximal at $t\to\infty$, when $\Delta T_c\to 0$. Note that neither ΔT_c nor ΔT_r depend on $T(R_b,t)\equiv T_s(t)$. The parameter ζ describes the relative contribution of the correction to T_{g0} due to thermal radiation.

Eq. (12) can be rewritten in an alternative form:

$$\dot q=\tilde h(T_{g0}-T_s) \tag{16}$$

where $\tilde h=\frac{k_g}{R_b}\chi$,

$$\chi=1+\frac{\Delta T_c+\Delta T_r}{T_{g0}-T_s} \tag{17}$$

In this case the factor χ describes the correction to h or k_g, which allows us to take into account the effect of transient heating of the body. This approach to the generalisation of Newton's law is similar to the one reported in [3], where it was assumed that the temperature of the body remains constant. The limitation of this approach is that the value of χ depends explicitly on $T_s(t)$. The series in Eq. (14) diverges at $t=0$ and $R=R_b$ due to the initial jump of temperature at the surface of the body, and cannot be used in the immediate vicinity of the point ($t=0$, $R=R_b$) due to poor convergence of the series.

Note that Eq. (16) can be obtained from the earlier mentioned solution by Cooper [5] ($R_g\to\infty$, $T(R,t)=\mathrm{const}$, no radiation) with χ given by the following formula:

$$\chi=\frac{-\frac{k_b}{k_g}\int_0^\infty\Phi(u)\exp(-u^2 Fo\frac{\kappa_b}{\kappa_g})\,\mathrm{d}u}{\int_0^\infty\frac{\sin u}{u\cos u-\sin u}\Phi(u)\exp(-u^2 Fo\frac{\kappa_b}{\kappa_g})\,\mathrm{d}u} \tag{18}$$

where

$$\Phi(u)=\frac{(u\cos u-\sin u)^2}{u^2\sin^2 u+\frac{\kappa_g}{\kappa_b}[\frac{k_b}{k_g}(u\cos u-\sin u)+\sin u]^2}$$

$Fo=t\kappa_g/R_b^2$ (Fourier number).

Before the analysis of the equations derived in this section for specific values of parameters is undertaken, they will be simplified in some limiting cases.

If $\varepsilon\equiv\sqrt{\frac{k_g c_{pg}\rho_g}{k_b c_b\rho_b}}\to 0$ then Eq. (9) can be simplified to:

$$\cot(\lambda a_b R_b)=\frac{k_b-k_g}{k_b a_b R_b\lambda} \tag{19}$$

The assumption $\varepsilon\to 0$ is equivalent to the assumption that $k_b\to\infty$. The latter assumption is widely used in engineering CFD codes describing particle and droplet heating. Also, the original assumption $\varepsilon\to 0$ could be supported by the fact that $\rho_b\gg\rho_g$.

The solution of Eq. (19) forms a countable set of increasing positive eigenvalues λ_n. In the limit $\lambda_n \to \infty$ this solution reduces to:

$$\lambda_n = \frac{(n+0.5)\pi}{a_b R_b} \tag{20}$$

In the case $\varepsilon \to 0$, series (10) converges absolutely and uniformly (see Appendix C).

In the case of a perfectly stirred gas, we can assume that its temperature is maintained everywhere equal to T_{g0} during the whole process of droplet heating. Ignoring the effect of thermal radiation, the solution of Eq. (2) for $0 \leqslant R \leqslant R_b$ with the boundary condition $T(R_b, t) = T_{g0}$ and initial condition $T(R, t=0) = T_{b0}$ can be presented as:

$$T(R,t) = T_{g0} + 2(T_{g0} - T_{b0}) \sum_{n=1}^{\infty} \frac{(-1)^n \sin \widetilde{R}_n}{\widetilde{R}_n} \times \exp\left[-\kappa_b \left(\frac{\pi n}{R_b}\right)^2 t\right] \tag{21}$$

where $\widetilde{R}_n = \pi n R/R_b$. Remembering that:

$$2\sum_{n=1}^{\infty} \frac{(-1)^n \sin \widetilde{R}_n}{\widetilde{R}_n} = -1$$

we can see that $T(R,t) \to T_{b0}$ when $t \to 0$. Also, $T(R,t) \to T_{g0}$ when $t \to \infty$, as expected.

Predictions of Eqs. (10) and (21) will be compared in the next section.

4. Analysis of the solution

The focus of the analysis of this section will be mainly on Eqs. (9), (10), (14), (15) and (16). Eq. (10) gives us the actual evolution of the distribution of temperature in the body and gas, while Eqs. (14), (15) and (16) allow us to estimate the limits of applicability of Newton's law of heating. All these equations use the eigenvalues λ_n obtained from Eq. (9). The analysis of these equations is simplified when the following dimensionless parameters are introduced for $T_{g0} > T_{b0}$:

$$\tilde{\lambda}_n = \lambda_n a_b R_b/\pi, \qquad \widetilde{R}_{(g)} = R_{(g)}/R_b$$
$$\widetilde{T} = (T_{g0} - T)/(T_{g0} - T_{b0})$$

$Fo_b = t\kappa_b/R_b^2$ (body Fourier number).

In the limit $\varepsilon \to 0$, λ_n are expected to be close to those determined by Eq. (20). This means that $\tilde{\lambda}_n$ in this case would be determined by a particularly simple expression:

$$\tilde{\lambda}_n = n + 0.5 \tag{22}$$

Let us consider typical values of parameters for the case when diesel fuel droplets with an initial temperature of 300 K are injected into a gas at temperature 800 K and pressure 30 atm (situation typical for diesel engines [16]):

$$\rho_b = 600\ \mathrm{kg\,m^{-3}}, \qquad k_b = 0.145\ \mathrm{W\,m^{-1}\,K^{-1}}$$
$$c_b = 2830\ \mathrm{J\,kg^{-1}\,K^{-1}}, \qquad \rho_g = 23.8\ \mathrm{kg\,m^{-3}}$$
$$k_g = 0.061\ \mathrm{W\,m^{-1}\,K^{-1}}, \qquad c_{pg} = 1120\ \mathrm{J\,kg^{-1}\,K^{-1}}$$

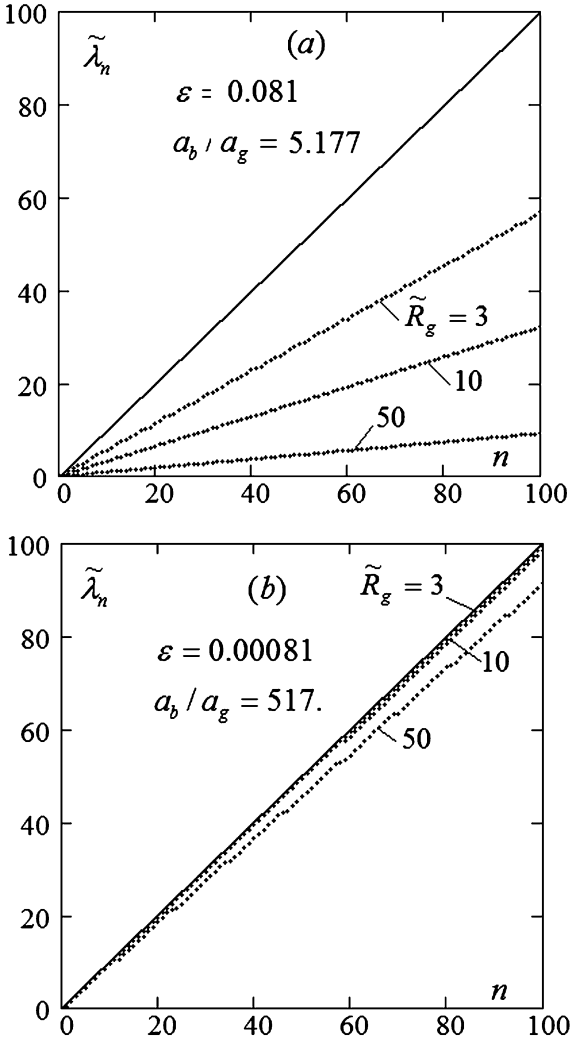

Fig. 1. Plots of $\tilde{\lambda}_n$ versus n based on Eq. (22) (solid) and the solution of Eq. (9) (dashed); numbers near the solid curves correspond to the values of $\widetilde{R}_g$; part (a) refers to $\varepsilon = 0.081$ and other values of parameters used in Section 4; part (b) refers to the same parameters as in (a), except that ε is assumed equal to 0.00081.

These parameters allow us to estimate $\varepsilon = 0.081$.

The plots of $\tilde{\lambda}_n$ versus n based on Eq. (9) for the values of parameters given above and $\widetilde{R}_g = 3$, 10 and 50 are presented in Fig. 1(a). In the same figure the line given by Eq. (22) is also presented. As can be seen from this figure, the values of $\tilde{\lambda}_n$ increase almost linearly with increasing n. For given n these values decrease with increasing $\widetilde{R}_g$. None of these properties of $\tilde{\lambda}_n$ seem to be at first evident from the observation of Eq. (9). Also, the values of $\tilde{\lambda}_n$ predicted by Eq. (9) seem to be rather different from those which follow from Eq. (22), especially for large $\widetilde{R}_g$. That means that $\varepsilon = 0.081$ is not small enough to justify the applicability of Eq. (22). In Fig. 1(b) the same plots as in Fig. 1(a) are presented but for $\varepsilon = 0.00081$. As follows from this figure, approximation (22) in this case appears to be reasonably good in the whole range of $\widetilde{R}_g$ under consideration.

Plots of $\widetilde{T}$ versus $\widetilde{R}$ for $\widetilde{R}_g = 3$ and $\widetilde{R}_g = 50$, and various Fo are shown in Fig. 2. Effects of thermal radiation are ignored. The plots for $\widetilde{R}_g > 50$ are indistinguishable from those

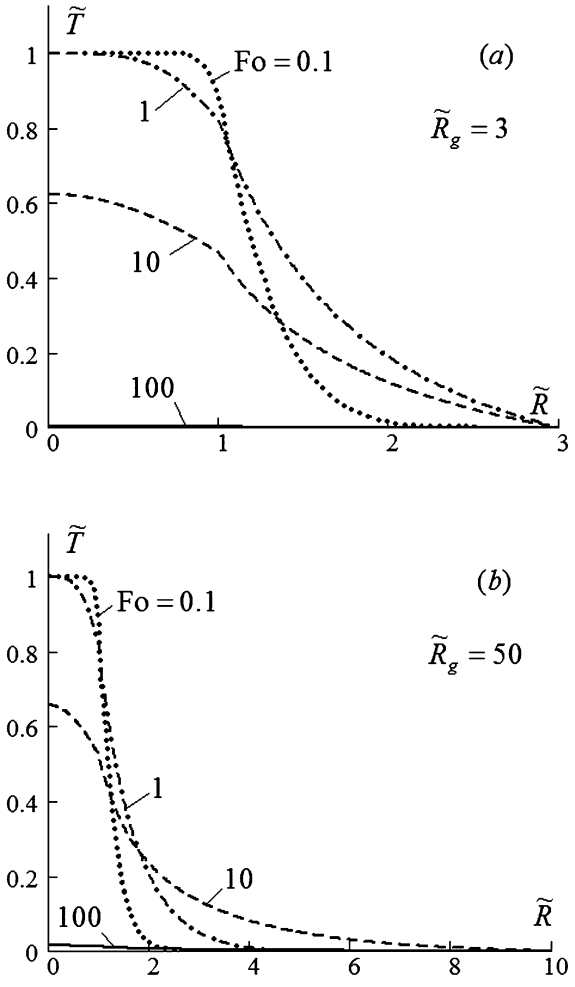

Fig. 2. Plots of $\widetilde{T}$ versus $\widetilde{R}$, based on Eq. (10), for $\widetilde{R}_g = 3$ (part (a)) and $\widetilde{R}_g = 50$ (part (b)), $n = 100$ and various Fo (numbers near the curves). The effect of thermal radiation is ignored.

for $\widetilde{R}_g = 50$ for the Fo under consideration. The Cesaro method of summation was used for numerical computation of the series for this and the following plots [38] (see Appendix D for the details). 100 terms in the series were used. Further increase of the number of terms did not change the results for the values of Fo under consideration. For $Fo < 0.1$, however, the convergence of the series deteriorated, and the solution turned out to be of limited practical use for these Fo. Considering values of parameters given earlier and $R_b = 10$ μm we obtain that $Fo = 0.1$ corresponds to

$$t = 0.1\frac{R_b^2}{\kappa_g} \approx 4.4\ \mu\text{s}$$

This time is much shorter than the typical time to heat-up droplets of this size (about 1 ms). Hence, the processes at $Fo < 0.1$ can be safely ignored in this application.

As follows from Fig. 2, for both values of $\widetilde{R}_g = 3$ and 50, and with $Fo = 0.1$, $\widetilde{T}$ drops rather quickly from 1 to almost zero when $\widetilde{R}$ increases from about 1 to 2. This corresponds to temperature increase from the one close to the initial body temperature T_{b0} to the initial gas temperature T_{g0}. The general 'flattening' of the curves for $Fo = 1$, $Fo = 10$ and $Fo = 100$ reflects the process of heating of the body and cooling of gas in the vicinity of droplets. The visible discontinuity of the derivative of $\widetilde{T}$ at $\widetilde{R} = 1$ is consistent with the boundary condition (6). The same discontinuity is present for other Fo, but it is less visible in the case of small and large derivatives of $\widetilde{T}$. At $Fo < 1$ gas cooling appears to be the dominant process, while at $Fo > 1$ the intensities of body heating and further gas cooling appear to be comparable. At $Fo = 100$ the process of body heating is almost complete, and the temperature of the body approaches the initial temperature of the surrounding gas. This process of body heating is slightly quicker for $\widetilde{R}_g = 3$ than for $\widetilde{R}_g = 50$. This result would be expected since in the case when $\widetilde{R}_g = 3$ the temperature at $\widetilde{R} = 3$ is maintained equal to T_{g0}, while in the case when $\widetilde{R}_g = 50$ the temperature at this level is allowed to drop due to transfer of heat from gas to the body. As follows from Fig. 2(b), the effect of the body on the gas becomes negligible at $\widetilde{R} > 10$ for all Fo. This is consistent with the estimate of the radius of the so-called cooling zone around the body, made in [3], based on a much more simplistic model, using the assumption that $T_s = \text{const}$. The size of the cooling zone is expected to decrease significantly when the body motion and the effects of mixing are taken into account. In the limiting case of perfectly stirred gas this cooling zone disappears altogether (see Eq. (21)). Note that the way of practical implementation of the model into the existing CFD codes is not at first evident. It is unclear how to make a distinction in the general case between the gas temperature in a computational cell, used in conventional CFD codes, and temperature $T(R_g)$, required for the implementation of the model. For small bodies and large cells these temperatures can be assumed the same.

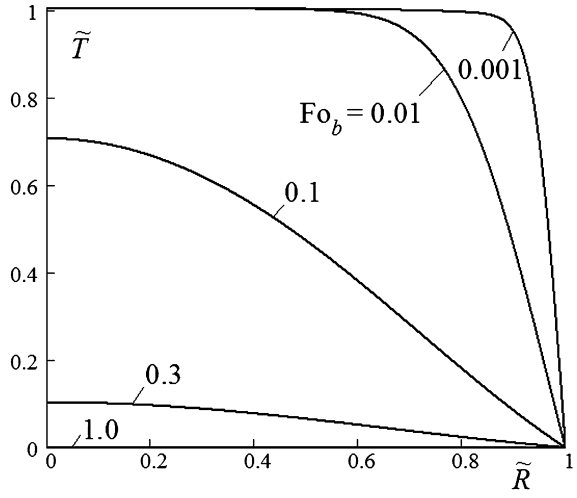

Fig. 3. The same plots as in Fig. 2, but for various Fo_b and based on Eq. (21) ($\widetilde{R}_g \to 1$).

The plots of $\widetilde{T}$ versus $\widetilde{R}$ based on Eq. (21) are shown in Fig. 3 for various Fo_b. For the values of parameters given above:

$$Fo_b = \frac{\kappa_b}{\kappa_g}Fo = \frac{k_b c_{pg}\rho_g}{k_g c_b \rho_b}Fo \approx 0.037Fo$$

These plots could be considered to be similar to those presented in Fig. 2(a), but for $\widetilde{R}_g \to 1$. Comparing the plots shown in Figs. 2 and 3, one can observe similarities in the temporal

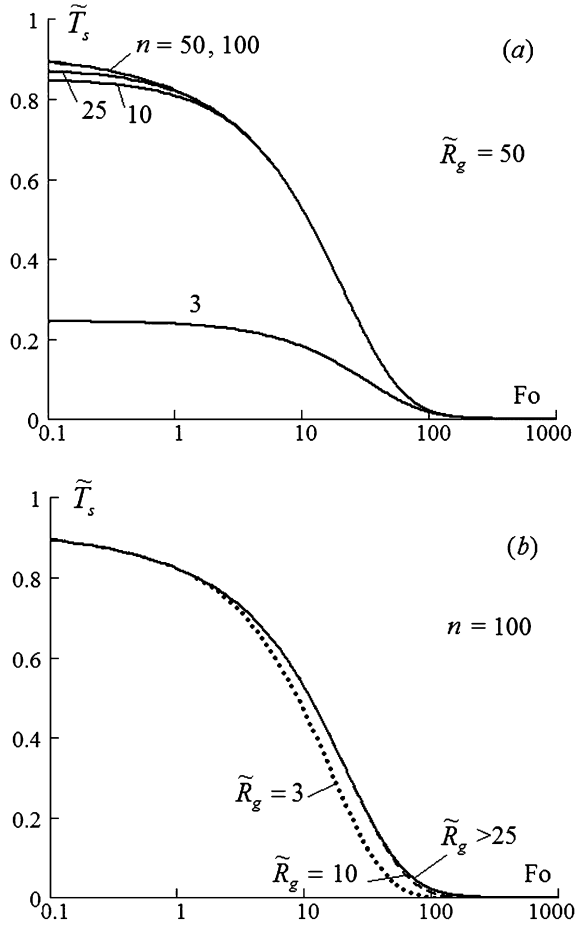

Fig. 4. Plots of $\widetilde{T}_s$ versus Fo for $\widetilde{R}_g = 50$ and $n = 3$, 10, 25, 50 and 100 (numbers near the curves) (a); plots of $\widetilde{T}_s$ versus Fo for $n = 100$ and $\widetilde{R}_g = 3$, 10 and > 25 (numbers near the curves) (b). The effect of thermal radiation is ignored.

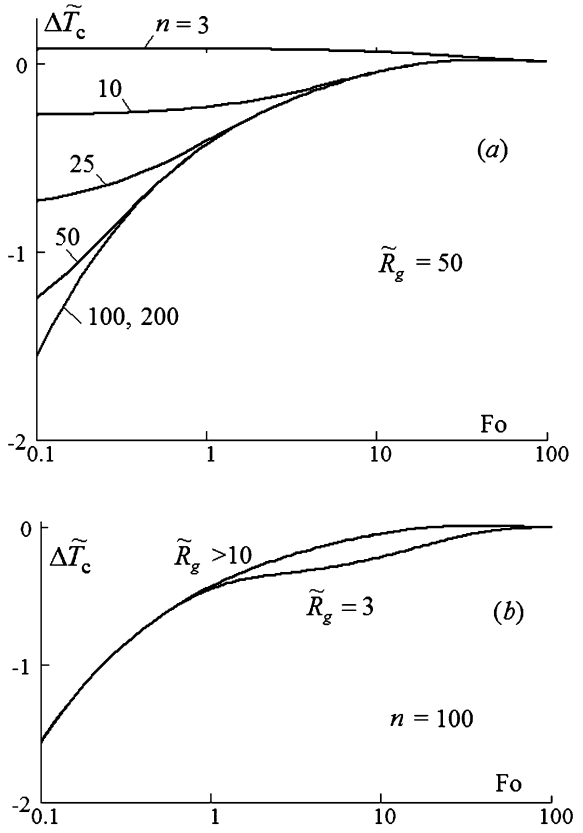

Fig. 5. Plots of $\Delta\widetilde{T}_c$ versus Fo for $\widetilde{R}_g = 50$ and $n = 3$, 10, 25, 50, 100 and 200 (numbers near the curves) (a); plots of $\Delta\widetilde{T}_c$ versus Fo for $n = 100$ and $\widetilde{R}_g = 3$ and > 10 (numbers near the curves) (b). The effect of thermal radiation is ignored.

evolution of $\widetilde{T}(\widetilde{R})$. There is, however, a noticeable difference between the curves, shown in Figs. 2 and 3. While in the cases shown in Fig. 2, the heating of the body is expected to be completed at $Fo = 100$, in the case shown in Fig. 3, this heating is expected to be completed at $Fo_b \approx 0.3$. The latter corresponds to $Fo \approx 0.3/0.037 \approx 10$. That means that in a well stirred gas, the heating of the body is expected to take place more than an order of magnitude faster when compared with the heating of the body in a quiescent gas. In real-life engineering applications the time required for a spherical body to heat-up is expected to be somewhere between the times corresponding to $Fo = 100$ and $Fo = 10$.

The plots of

$$\widetilde{T}_s = \big(T_{g0} - T_b(R = R_b)\big)/(T_{g0} - T_{b0})$$

versus Fo for $\widetilde{R}_g = 50$ and various numbers of terms n taken in the series are shown in Fig. 4(a). In Fig. 4(b) the same plots as in Fig. 4(a) are shown but for $n = 100$ and various $\widetilde{R}_g$. As follows from Fig. 4(a), $n = 100$ appears to be sufficient to obtain an accurate solution in the whole range of Fo from 0.1 to 1000. If we were interested just in $Fo > 10$ then 10 terms of the series would have been sufficient; for $Fo > 100$ we could take $n = 3$. As follows from Fig. 4(b), the curves corresponding to $\widetilde{R}_g = 10$ are almost indistinguishable from the curves corresponding to higher $\widetilde{R}_g$. This result is consistent with our previous conclusion that the influence of the body on the gas temperature does not penetrate beyond $\widetilde{R} = 10$. Both sets of Figs. 4(a), (b) predict that $\widetilde{T}_s$ is close to 0.9 for $Fo = 0.1$. This result is consistent with Figs. 2(a), (b), and indicates that the change of body surface temperature is clearly visible even for rather short times corresponding to $Fo = 0.1$. At times corresponding to $Fo < 0.1$ the convergence of the series deteriorates, and more than 100 terms would be required to describe adequately the properties of $\widetilde{T}_s$. This limitation, however, would have limited impact in practical situations, as we are not generally interested in the initial heating of the body ($t < 4.4$ μs in the case of the droplets considered earlier).

The plots similar to those presented in Figs. 4(a), (b), but for

$$\Delta\widetilde{T}_c = -\Delta T_c/(T_{g0} - T_{b0})$$

(see Eqs. (13) and (14)) are shown in Figs. 5(a), (b). As follows from Fig. 5(a), for $Fo = 0.1$ the curves corresponding to $n = 100$ are practically indistinguishable from the curves corresponding to $n = 200$. For $Fo \geqslant 10$ ten terms in the series predict the result which is indistinguishable from the case when more terms in the series are taken into account. As follows from Fig. 5(b), the plots for $n = 100$ and $\widetilde{R}_g = 10$ are indistinguishable from the plots for $n = 100$ and $\widetilde{R}_g > 10$. Hence, the case of $\widetilde{R}_g = 10$ can be considered to be a good approximation for the case when a body is immersed into an infinitely large pool

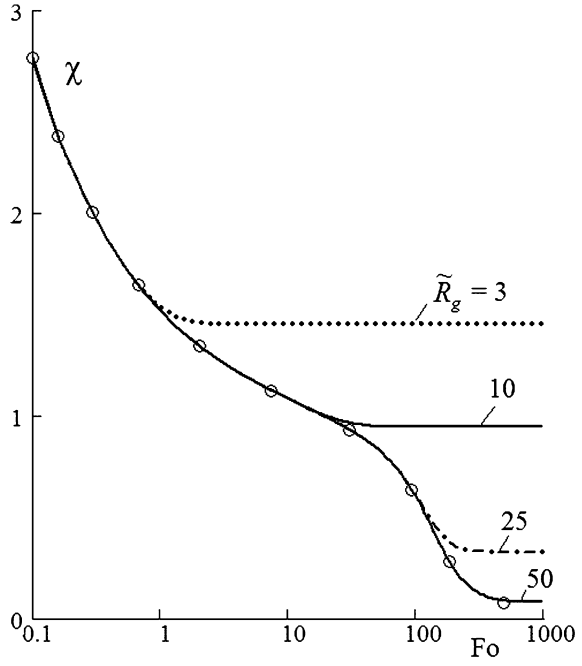

Fig. 6. Plots of χ versus Fo for various $\widetilde{R}_g$ (numbers near the curves). Effects of radiation are ignored and 100 terms in the series were taken. The results predicted by Eq. (18) are shown by circles.

of fluid at the initial temperature T_{g0} (cf. the analysis of Figs. 2 and 4). Note that the curve corresponding to $n = 3$ in Fig. 5(a) predicts an unphysical solution $\Delta\widetilde{T}_c > 0$ for small Fo. Hence, this number of terms is not sufficient for an adequate description of the heat transfer from gas to droplets.

As follows from Figs. 5(a), (b), $\Delta\widetilde{T}_c \approx -1.6$ at $Fo = 0.1$. This means that we can use Newton's law for this Fo if we replace the gas temperature T_{g0} by $T_{\text{eff}} = T_{g0} + 1.6(T_{g0} - T_{b0})$ (see Eq. (13)). The latter value is generally significantly larger than T_{g0}. For small T_{b0} the modified Newton's law predicts a heat transfer rate about 2.6 times larger than the conventional Newton's law. The value of $\Delta\widetilde{T}_c$ increases rather quickly with increasing Fo. For $Fo = 1$ we have $\Delta\widetilde{T}_c \approx -0.5$, while for $Fo = 10$ we have $\Delta\widetilde{T}_c \approx -0.1$. However, even in this case the application of the conventional Newton's law might be not justified. This can be illustrated via rewriting Eq. (12) in the form:

$$\dot{q} = h\big[T_{\text{eff}} - T(R_b, t)\big] = h\big[T_{g0} - T_s(t) - \Delta\widetilde{T}_c(T_{g0} - T_{b0})\big] \tag{23}$$

As follows from this equation, the smallness of $\Delta\widetilde{T}_c$ does not imply that the term proportional to $\Delta\widetilde{T}_c$ can be ignored. Indeed, as follows from Fig. 4, $T_{g0} - T_s(t)$ always approaches zero for large Fo. Hence we might expect that the term $T_{g0} - T_s(t)$ in Eq. (23) can eventually become less than the term $\Delta\widetilde{T}_c(T_{g0} - T_{b0})$ for sufficiently large Fo. A more reliable way to estimate the range of applicability of Newton's law could be based on Eq. (16).

The plots of $\chi(Fo)$ for the same values of parameters as in Fig. 5(b) are shown in Fig. 6. As follows, from this figure, χ decreases from about 2.8 to about 1.5 when Fo increases from 0.1 to 1 for all $\widetilde{R}_g$ under consideration. At larger Fo the dependence $\chi(Fo)$ becomes a rather sensitive function of $\widetilde{R}_g$. For $\widetilde{R}_g = 3$, χ remains almost constant and equal to 1.5 at $Fo > 1$. For $\widetilde{R}_g = 10$, χ decreases with increasing Fo, until $Fo \approx 20$ and then remains almost constant and equal to 1. For $\widetilde{R}_g \geqslant 50$, χ approaches zero for large Fo, which indicates the decrease of heat transfer, compared with the one predicted by Newton's law. The practical importance of this range of Fo, however, is limited as here the heat transfer from gas to droplets is negligible (see the discussion of Fig. 5). On the same figure the results predicted by the model developed in [5] (Eq. (18)) are shown. As expected, the values of χ predicted by both Eq. (17) for $\widetilde{R}_g = 50$ and Eq. (18) for $\widetilde{R}_g = \infty$ are practically indistinguishable. This confirms the validity of ours and Copper's [5] solutions for large $\widetilde{R}_g$. If the body surface temperature was fixed then $\chi \to 1$ when $Fo \to \infty$ and $R_g \to \infty$ [2–4].

Some results shown in Figs. 5(b) and 6 could be understood based on the underlying physics of the processes. At small Fo the body exchanges heat only with the gas in the immediate vicinity of droplets. Hence, the values of $\widetilde{T}$ and χ are not affected by R_g (see Fig. 2). This is consistent with absence of any visible dependence of χ on $\widetilde{R}_g$ in the plots shown in Fig. 6. For larger Fo, however, more and more remote areas of gas become involved in heat exchange with droplets, and here the dependence of the heat transfer on $\widetilde{R}_g$ becomes important. For example, for $\widetilde{R}_g = 50$ the value of $\widetilde{T}$ at $\widetilde{R} = 3$ becomes equal to about 0.15 for $Fo = 10$. This corresponds to $T \approx 0.85T_{g0} + 0.15T_{b0} < T_{g0}$. At the same time, for $\widetilde{R}_g = 3$ the value of T at $\widetilde{R} = 3$ is maintained equal to T_{g0}. Hence, heat transfer from gas to droplets is expected to be stronger at $\widetilde{R}_g = 3$ than at $\widetilde{R}_g = 50$, which is consistent with the prediction of Fig. 6.

Finally, the effect of thermal radiation will be investigated. We consider two cases: relatively weak radiation corresponding to $\theta_R = T_{\text{ext}} = 800$ K, and strong radiation corresponding to $\theta_R = T_{\text{ext}} = 2000$ K. Following [32], we assume that liquid is low sulfur ESSO AF1313 diesel fuel and parameters a and b are calculated from the following formulae:

$$a = \big[0.10400 - 0.054320\theta_R/1000 + 0.008(\theta_R/1000)^2\big] \times 10^{6b}$$

$$b = 0.49162 + 0.098369\theta_R/1000 - 0.007857(\theta_R/1000)^2$$

Note that the original values of a given in [32] for R_d measured in μm have been adjusted to our case where R_d is measured in m. Other values of parameters are the same as before. The calculations are performed based on Eqs. (13) and (17) taking into account both conductive and radiation terms.

Plots of ζ versus Fo for $\widetilde{R}_g = 3$ and $\widetilde{R}_g = 50$ are shown in Figs. 7(a), (b). In all cases $\zeta \to \infty$ when $Fo \to \infty$, and ζ increases with increasing Fo. This increase of ζ is monotonous in the whole range of Fo under consideration in the case of $\widetilde{R}_g = 3$. In the case of $\widetilde{R}_g = 50$ a singularity at about $Fo = 20$ is predicted for both external temperatures (not shown in the figure). This singularity is related to the fact that ΔT_c is equal to zero in the vicinity of this point, which corresponds to the case $\chi = 1$. As expected, the effect of thermal radiation is stronger for $T_{\text{ext}} = 2000$ K than for $T_{\text{ext}} = 800$ K. Positive values of ζ for $\Delta T_c > 0$ indicate that the thermal radiation provides an additional heating of the body. The condition $\Delta T_c > 0$ is equivalent to the condition $\chi > 1$ (see Fig. 6).

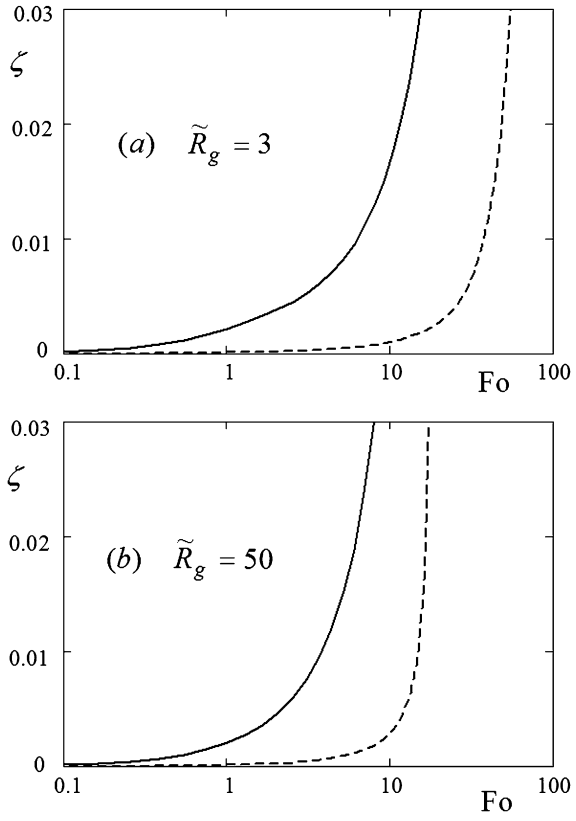

Fig. 7. Plots of ζ versus Fo for $T_{\text{ext}} = 2000$ K (solid curves) and $T_{\text{ext}} = 800$ K (dashed curves) for $\widetilde{R}_g = 3$ (a) and $\widetilde{R}_g = 50$ (b). T_{ext} describes the effect of thermal radiation.

Note that thermal radiation controls not only ζ, but also the value of the body surface temperature. To investigate this effect, the following dimensionless parameter is introduced:

$$\xi = \frac{T_{g0} - T_{s(r)}}{T_{g0} - T_{s(c)}}$$

where $T_{s(r)}$ is the body surface temperature, calculated in the presence of thermal radiation, $T_{s(c)}$ is the body surface temperature, when the effect of thermal radiation is ignored. The plots of ξ versus *Fo* for the same values of parameters as in Figs. 7(a), (b) are shown in Figs. 8(a), (b). As follows from this figure, ξ is close to 1 for small *Fo*, but decreases monotonically with increasing *Fo*. This means that the effect of thermal radiation accelerates the approach of the body surface temperature to T_{g0} as expected. This effect is particularly important for large *Fo*, when the difference between these temperatures becomes small.

Finally the comparison between the plots of χ versus *Fo*, in the presence and in the absence of radiation, is shown in Fig. 9. In agreement with Figs. 7 and 8, the effect of thermal radiation on χ is small for small *Fo*, and increases with increasing *Fo*. The sign of the radiative correction to χ depends on whether $\chi > 1$ or $\chi < 1$. In the first case the radiative corrections lead to an increase of χ, while in the second case they lead to its decrease. In both cases $\Delta T_r > 0$. These results are consistent with the prediction of Fig. 8.

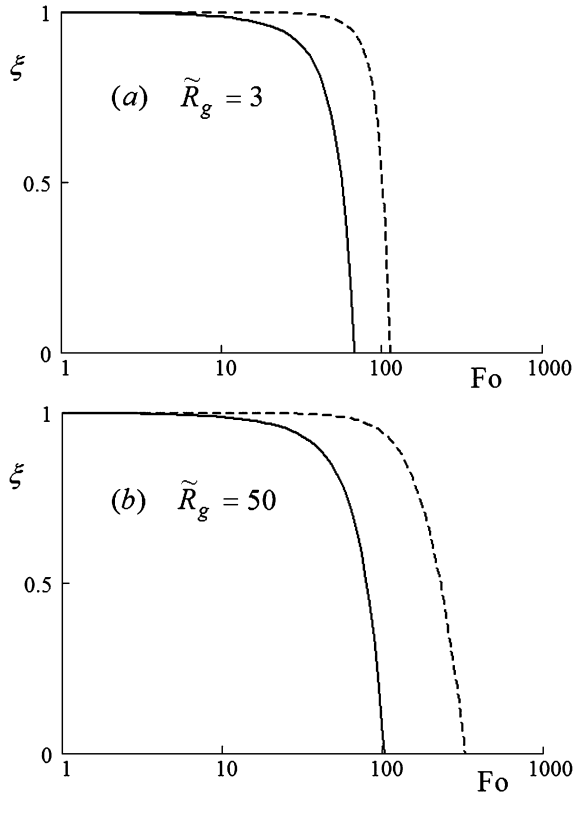

Fig. 8. The same as Fig. 7, but for the parameter ξ.

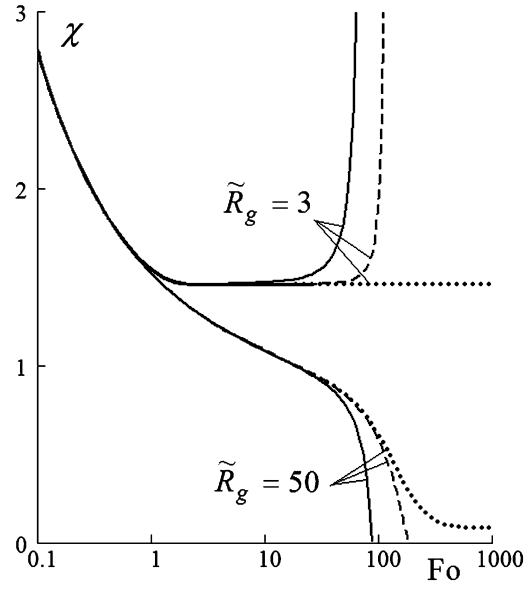

Fig. 9. Plots of χ versus *Fo* for various $\widetilde{R}_g$ (numbers near the curves) in the presence of thermal radiation. Dotted curves refer to the case without radiation dashed curves refer to $T_{\text{ext}} = 800$ K, solid curves refer to $T_{\text{ext}} = 2000$ K.

5. Conclusions

The problem of transient heating of a stationary semitransparent spherical body immersed in a stationary hot gas in the presence of thermal radiation has been investigated. The size of the domain occupied by the gas has been assumed to be finite, and the outer boundary of this domain has been kept at

constant temperature. The initial radial distribution of temperature in the body has been taken into account in the general solution. Assuming that the body is stationary and the effects of natural convection can be ignored, the conventional Newton law of body heating has been generalised by introducing a correction for the initial gas temperature or convective heat transfer coefficient. Explicit expressions for these corrections have been obtained. The results have been analysed for values of parameters relevant to diesel engines.

It has been pointed out that in the absence of radiation the correction to the gas temperature decreases from about 1.6 of the difference between the initial gas and droplet temperatures at gas Fourier number $Fo = 0.1$ to about 0.1 of this difference for $Fo = 10$ and $R_g \geqslant 10$, or to about 0.3 of this difference for $Fo = 10$ and $R_g = 3$. For large Fo, this correction is expected to be of limited practical importance, as both this correction and the difference between the initial gas temperature and the body surface temperature approach zero (heat transferred from gas to the body becomes negligible).

The correction of the convective heat transfer coefficient has led to essentially the same conclusions as the correction of gas temperature. For small Fo, this correction does not depend on the size of the domain, and reaches about 2.8 at $Fo = 0.1$. For $Fo > 1$ this correction becomes sensitive to the size of the domain. For large domains it has been shown to be the same as follows from the earlier model suggested in [5] for an infinitely large domain occupied by the gas. The values of this correction to Newton's law vary from about 0.1 (large domain occupied by gas and $Fo = 500$) to 2.8 at $Fo = 0.1$. This means that ignoring these corrections is expected to lead to unacceptably large errors in computations.

The body heating process is expected to be almost completed at times corresponding to $Fo = 100$. This is more than an order of magnitude longer than the time required for the same body heating in a perfectly stirred gas, in which the body surface temperature is maintained equal to the initial gas temperature.

The effect of thermal radiation on droplet heating has been accounted for via additional corrections of the initial gas temperature and the convection heat transfer coefficient. It has been pointed out that for the parameters typical for diesel engines, these corrections are negligibly small for small Fo, but can become significant for large Fo. In the latter case, however, the overall heat transfer process becomes very weak.

A number of simplifications of the model (e.g. ignoring the effects of evaporation and temperature dependence of physical parameters) limits the range of its direct applications. In the case of diesel engines, this model can be considered as a base for development of a more comprehensive model. The present version of the model can illustrate the contribution of the transient effects on diesel droplet heating at a qualitative level.

Appendix A. Derivation of formula (7)

Introducing a new variable

$$u = (T - T_{g0})R$$

we can simplify Eq. (2) and initial and boundary conditions (5)–(6) to:

$$\frac{\partial u}{\partial t} = \kappa \frac{\partial^2 u}{\partial R^2} + R P(t, R) \tag{A.1}$$

$$u|_{t=0} = \begin{cases} -T_0 R & \text{when } R \leqslant R_b \\ 0 & \text{when } R_b < R \leqslant R_g \end{cases} \tag{A.2}$$

$$\begin{aligned} &u|_{R=R_b^-} = u|_{R=R_b^+} \\ &k_b[R_b u'_R - u]|_{R=R_b^-} = k_g[R_b u'_R - u]|_{R=R_b^+} \\ &u|_{R=R_g} = 0, \end{aligned} \tag{A.3}$$

where $T_0 \equiv T_0(R) = T_{g0} - T_{b0}(R)$ depends on R in the general case.

Conditions (A.3) need to be amended by the boundary condition at $R = 0$. Since $T - T_{g0}$ is finite at $R = 0$ then $u|_{R=0} = 0$.

We look for the solution of Eq. (A.1) in the form:

$$u = \sum_{n=1}^{\infty} \Theta_n(t) v_n(R) \tag{A.4}$$

where functions $v_n(R)$ form the full set of non-trivial solutions of the eigenvalue problem:

$$\frac{\mathrm{d}^2 v}{\mathrm{d}R^2} + a^2 \lambda^2 v = 0 \tag{A.5}$$

subject to boundary conditions:

$$\begin{aligned} &v|_{R=0} = v|_{R=R_g} = 0 \\ &v|_{R=R_b^-} = v|_{R=R_b^+} \\ &k_b[R_b v'_R - v]|_{R=R_b^-} = k_g[R_b v'_R - v]|_{R=R_b^+} \end{aligned} \tag{A.6}$$

where

$$a = \frac{1}{\sqrt{\kappa}} = \begin{cases} \sqrt{\frac{c_b \rho_b}{k_b}} \equiv a_b & \text{when } R \leqslant R_b \\ \sqrt{\frac{c_{pg} \rho_g}{k_g}} \equiv a_g & \text{when } R_b < R \leqslant R_g \end{cases} \tag{A.7}$$

Note that λ has dimension $1/\sqrt{\text{time}}$. We look for the solution of Eq. (A.5) in the form:

$$v(R) = \begin{cases} A \sin(\lambda a_b R) & \text{when } R \leqslant R_b \\ B \sin(\lambda a_g (R - R_g)) & \text{when } R_b < R \leqslant R_g \end{cases} \tag{A.8}$$

Function (A.8) satisfies boundary conditions (A.6) at $R = 0$. Having substituted function (A.8) into boundary conditions (A.6) at $R = R_b$ we obtain:

$$A \sin(\lambda a_b R_b) = B \sin\big(\lambda a_g (R_b - R_g)\big) \tag{A.9}$$

$$\begin{aligned} &A k_b \big[R_b \lambda a_b \cos(\lambda a_b R_b) - \sin(\lambda a_b R_b)\big] \\ &\quad = B k_g \big[R_b \lambda a_g \cos\big(\lambda a_g (R_b - R_g)\big) \\ &\qquad - \sin\big(\lambda a_g (R_b - R_g)\big)\big] \end{aligned} \tag{A.10}$$

Condition (A.9) is satisfied when:

$$\left.\begin{aligned} A &= [\sin(\lambda a_b R_b)]^{-1} \\ B &= [\sin(\lambda a_g (R_b - R_g))]^{-1} \end{aligned}\right\} \tag{A.11}$$

Having substituted Eqs. (A.11) into (A.10) we obtain:

$$k_b\big[R_b\lambda a_b\cot(\lambda a_b R_b)-1\big] = k_g\big[R_b\lambda a_g\cot\big(\lambda a_g(R_b-R_g)\big)-1\big] \quad (A.12)$$

Remembering the definitions of a_b and a_g, Eq. (A.12) can be simplified to:

$$\sqrt{k_b c_b\rho_b}\cot(\lambda a_b R_b)-\sqrt{k_g c_{pg}\rho_g}\cot\big(\lambda a_g(R_b-R_g)\big) = \frac{k_b-k_g}{R_b\lambda} \quad (A.13)$$

Eq. (A.13) allows us to find a countable set of positive eigenvalues λ_n [39] which can be arranged in ascending order $0<\lambda_1<\lambda_2<\cdots$. Note that the negative solutions $-\lambda_n$ also satisfy Eq. (A.13) as both sides of this equation are odd functions of λ. $\lambda=0$, however, does not satisfy this equation. Having substituted these values of λ_n into Eq. (A.8) and remembering Eqs. (A.11) we obtain the expressions for eigenfunctions v_n in the form:

$$v_n(R)=\begin{cases}\frac{\sin(\lambda_n a_b R)}{\sin(\lambda_n a_b R_b)} & \text{when } R\leqslant R_b\\ \frac{\sin(\lambda_n a_g(R-R_g))}{\sin(\lambda_n a_g(R_b-R_g))} & \text{when } R_b<R\leqslant R_g\end{cases} \quad (A.14)$$

It can be shown (see Appendix B) that functions $v_n(R)$ are orthogonal with weight

$$b=\begin{cases}k_b a_b^2=c_b\rho_b & \text{when } R\leqslant R_b\\ k_g a_g^2=c_{pg}\rho_g & \text{when } R_b<R\leqslant R_g\end{cases}$$

This means that: $\int_0^{R_g} v_n(R)v_m(R)b\,\mathrm{d}R=\delta_{nm}\|v_n\|^2$, where

$$\delta_{nm}=\begin{cases}1 & \text{when } n=m\\ 0 & \text{when } n\neq m\end{cases}$$

The proof of completeness of this set of functions is much more complicated (it is based on the methods of functional analysis and properties of Banach spaces [40]). Implicitly, the fact that this set is complete, could be supported by the agreement between our results and those of Cooper [5], as mentioned earlier.

The norm of v_n with weight b is calculated as:

$$\begin{aligned}\|v_n\|^2 &= \int_0^{R_g} v_n^2 b\,\mathrm{d}R\\ &= \int_0^{R_b}\left[\frac{\sin(\lambda_n a_b R)}{\sin(\lambda_n a_b R_b)}\right]^2 c_b\rho_b\,\mathrm{d}R\\ &\quad+\int_{R_b}^{R_g}\left[\frac{\sin(\lambda_n a_g(R-R_g))}{\sin(\lambda_n a_g(R_b-R_g))}\right]^2 c_{pg}\rho_g\,\mathrm{d}R\\ &= \frac{c_b\rho_b}{2\sin^2(\lambda_n a_b R_b)}\left[R_b-\frac{\sin(2\lambda_n a_b R_b)}{2\lambda_n a_b}\right]\\ &\quad+\frac{c_{pg}\rho_g}{2\sin^2(\lambda_n a_g(R_b-R_g))}\\ &\quad\times\left[R_g-R_b+\frac{\sin(2\lambda_n a_b(R_b-R_g))}{2\lambda_n a_g}\right]\\ &= \frac{c_b\rho_b R_b}{2\sin^2(\lambda_n a_b R_b)}+\frac{c_{pg}\rho_g(R_g-R_b)}{2\sin^2(\lambda_n a_g(R_b-R_g))}\\ &\quad-\frac{k_b-k_g}{2R_b\lambda_n^2}\end{aligned} \quad (A.15)$$

When deriving Eq. (A.15) we took into account Eq. (A.13). Since all functions v_n satisfy boundary conditions (A.6), function u defined by expression (A.4) satisfies boundary conditions (A.3). Let us expand $RP(t,R)$ in a series over v_n:

$$RP(t,R)=\sum_{n=1}^{\infty} p_n(t)v_n(R) \quad (A.16)$$

where:

$$p_n(t)=\frac{1}{\|v_n\|^2}\int_0^{R_g} RP(t,R)v_n(R)b\,\mathrm{d}R$$

Remembering that $P(t,R)=0$ at $R>R_b$ the latter formula can be simplified to:

$$p_n(t)=\frac{c_b\rho_b}{\|v_n\|^2}\int_0^{R_b} RP(t,R)v_n(R)\,\mathrm{d}R$$

Having substituted Eqs. (A.4) and (A.16) into Eq. (A.1)) we obtain:

$$\sum_{n=1}^{\infty}\Theta_n'(t)v_n(R) = -\sum_{n=1}^{\infty}\Theta_n(t)\lambda_n^2 v_n(R)+\sum_{n=1}^{\infty}p_n(t)v_n(R) \quad (A.17)$$

When deriving Eq. (A.17) we took into account that functions $v_n(R)$ satisfy Eq. (A.5) for $\lambda=\lambda_n$. Eq. (A.17) is satisfied if and only if:

$$\Theta_n'(t)=-\lambda_n^2\Theta_n(t)+p_n(t) \quad (A.18)$$

The initial condition for $\Theta_n(t)$ can be obtained after substituting expression (A.4) into initial condition (A.2) for u:

$$\sum_{n=1}^{\infty}\Theta_n(0)v_n(R)=\begin{cases}-T_0R & \text{when } R\leqslant R_b\\ 0 & \text{when } R_b<R\leqslant R_g\end{cases} \quad (A.19)$$

Remembering the orthogonality of v_n with the weight b, we obtain from Eq. (A.19):

$$\Theta_n(0)=\frac{1}{\|v_n\|^2}\int_0^{R_b}(-T_0R)v_n(R)b\,\mathrm{d}R$$

If $T_0=\text{const}$ then this equation can be further simplified to:

$$\begin{aligned}\Theta_n(0) &= -\frac{c_b\rho_b T_0}{\|v_n\|^2\sin(\lambda_n a_b R_b)}\int_0^{R_b} R\sin(\lambda_n a_b R)\,\mathrm{d}R\\ &= \frac{T_0\sqrt{k_b c_b\rho_b}}{\lambda_n\|v_n\|^2}\left[R_b\cot(\lambda_n a_b R_b)-\frac{1}{\lambda_n a_b}\right]\end{aligned} \quad (A.20)$$

The solution of Eq. (A.18) subject to the initial condition (A.20) can be written as:

$$\Theta_n(t) = \exp\bigl(-\lambda_n^2 t\bigr)\Theta_n(0) + \int_0^t \exp\bigl(-\lambda_n^2(t-\tau)\bigr)p_n(\tau)\,\mathrm{d}\tau \tag{A.21}$$

Eq. (7) follows from the definition of u and Eqs. (A.4) and (A.21).

Appendix B. Proof of orthogonality of $v_n(R)$ with the weight b

Remembering expressions (A.14) for $v_n(R)$ we can write for $n \neq m$:

$$\begin{aligned}
I_{nm} &\equiv \int_0^{R_g} v_n(R)v_m(R)b\,\mathrm{d}R \\
&= \frac{k_b a_b^2}{\sin(\lambda_n a_b R_b)\sin(\lambda_m a_b R_b)} \\
&\quad\times \int_0^{R_b} \sin(\lambda_n a_b R)\sin(\lambda_m a_b R)\,\mathrm{d}R \\
&\quad + \frac{k_g a_g^2}{\sin(\lambda_n a_g(R_b-R_g))\sin(\lambda_m a_g(R_b-R_g))} \\
&\quad\times \int_{R_b}^{R_g} \sin\bigl(\lambda_n a_g(R-R_g)\bigr)\sin\bigl(\lambda_m a_g(R-R_g)\bigr)\,\mathrm{d}R \\
&= \frac{k_b a_b^2}{2\sin(\lambda_n a_b R_b)\sin(\lambda_m a_b R_b)} \\
&\quad\times \left[\frac{\sin((\lambda_n-\lambda_m)a_b R_b)}{(\lambda_n-\lambda_m)a_b} - \frac{\sin((\lambda_n+\lambda_m)a_b R_b)}{(\lambda_n+\lambda_m)a_b}\right] \\
&\quad - \frac{k_g a_g^2}{2\sin(\lambda_n a_g(R_b-R_g))\sin(\lambda_m a_g(R_b-R_g))} \\
&\quad\times \left[\frac{\sin((\lambda_n-\lambda_m)a_g(R_b-R_g))}{(\lambda_n-\lambda_m)a_g}\right. \\
&\quad \left. - \frac{\sin((\lambda_n+\lambda_m)a_g(R_b-R_g))}{(\lambda_n+\lambda_m)a_g}\right] \\
&= \frac{1}{2(\lambda_n-\lambda_m)}\left[\frac{k_b a_b \sin((\lambda_n-\lambda_m)a_b R_b)}{\sin(\lambda_n a_b R_b)\sin(\lambda_m a_b R_b)}\right. \\
&\quad \left. - \frac{k_g a_g \sin((\lambda_n-\lambda_m)a_g(R_b-R_g))}{\sin(\lambda_n a_g(R_b-R_g))\sin(\lambda_m a_g(R_b-R_g))}\right] \\
&\quad + \frac{1}{2(\lambda_n+\lambda_m)}\left[-\frac{k_b a_b \sin((\lambda_n+\lambda_m)a_b R_b)}{\sin(\lambda_n a_b R_b)\sin(\lambda_m a_b R_b)}\right. \\
&\quad \left. + \frac{k_g a_g \sin((\lambda_n+\lambda_m)a_g(R_b-R_g))}{\sin(\lambda_n a_g(R_b-R_g))\sin(\lambda_m a_g(R_b-R_g))}\right] \\
&= \bigl[k_b a_b\bigl(\cot(\lambda_m a_b R_b) - \cot(\lambda_n a_b R_b)\bigr) \\
&\quad - k_g a_g\bigl(\cot\bigl(\lambda_m a_b(R_b-R_g)\bigr) - \cot\bigl(\lambda_n a_b(R_b-R_g)\bigr)\bigr)\bigr] \\
&\quad\times \bigl[2(\lambda_n-\lambda_m)\bigr]^{-1} \\
&\quad + \bigl[-k_b a_b\bigl(\cot(\lambda_m a_b R_b) + \cot(\lambda_n a_b R_b)\bigr) \\
&\quad + k_g a_g\bigl(\cot\bigl(\lambda_m a_b(R_b-R_g)\bigr) + \cot\bigl(\lambda_n a_b(R_b-R_g)\bigr)\bigr)\bigr] \\
&\quad\times \bigl[2(\lambda_n+\lambda_m)\bigr]^{-1}
\end{aligned}$$

Remembering Eq. (A.13) we can write:

$$\begin{aligned}
I_{nm} &= \frac{1}{2(\lambda_n-\lambda_m)}\left(\frac{k_b-k_g}{R_b\lambda_m} - \frac{k_b-k_g}{R_b\lambda_n}\right) \\
&\quad - \frac{1}{2(\lambda_n+\lambda_m)}\left(\frac{k_b-k_g}{R_b\lambda_m} + \frac{k_b-k_g}{R_b\lambda_n}\right) \\
&= \frac{k_b-k_g}{2R_b\lambda_n\lambda_m} - \frac{k_b-k_g}{2R_b\lambda_n\lambda_m} = 0
\end{aligned}$$

Appendix C. Proof of convergence of the series in (10) in the limit $\varepsilon \to 0$

Remembering (20) we can expect that $(k_b-k_g)/(2R_b\lambda_n^2)$ is less than any *a priori* chosen constant for sufficiently large n ($n > N$). Having chosen this constant equal to $c_b\rho_b R_b/4$ we can write:

$$\frac{k_b-k_g}{2R_b\lambda_n^2} \leqslant \frac{c_b\rho_b R_b}{4\sin^2(\lambda_n a_b R_b)}$$

for $n > N$ and $k_b > k_g$.

Remembering this estimate and expression (A.15) for $\|v_n\|^2$ we obtain:

$$\|v_n\|^2|_{n>N} \geqslant \frac{c_b\rho_b R_b}{4\sin^2(\lambda_n a_b R_b)} + \frac{c_{pg}\rho_g(R_g-R_b)}{2\sin^2(\lambda_n a_g(R_b-R_g))}$$

This inequality can be inverted to:

$$\begin{aligned}
\frac{1}{\|v_n\|^2}|_{n>N} &\leqslant \bigl[4\sin^2(\lambda_n a_b R_b)\sin^2\bigl(\lambda_n a_g(R_b-R_g)\bigr)\bigr] \\
&\quad\times \bigl[c_b\rho_b R_b \sin^2\bigl(\lambda_n a_g(R_b-R_g)\bigr) \\
&\quad + 2c_{pg}\rho_g(R_g-R_b)\sin^2(\lambda_n a_b R_b)\bigr]^{-1}
\end{aligned} \tag{C.1}$$

Since the denominator in Eq. (C.1) is the sum of positive terms we can rearrange the estimate (C.1) to:

$$\frac{1}{\|v_n\|^2}|_{n>N} \leqslant \begin{cases} \frac{4\sin^2(\lambda_n a_b R_b)}{c_b\rho_b R_b} & \text{when } 0 \leqslant R \leqslant R_b \\ \frac{2\sin^2(\lambda_n a_g(R_b-R_g))}{c_{pg}\rho_g(R_g-R_b)} & \text{when } R_b < R \leqslant R_g \end{cases} \tag{C.2}$$

With a view of Eq. (A.14) and inequality (C.2) we have the following estimate:

$$\begin{aligned}
\frac{|v_n(R)|}{\|v_n\|^2}|_{n>N} &\leqslant \left\{\begin{array}{ll} \frac{4}{c_b\rho_b R_b} & \text{when } 0 \leqslant R \leqslant R_b \\ \frac{2}{c_{pg}\rho_g(R_g-R_b)} & \text{when } R_b < R \leqslant R_g \end{array}\right\} \\
&\leqslant \text{const}_1
\end{aligned} \tag{C.3}$$

This allows us to make the following estimate for sufficiently large n:

$$\begin{aligned}
\bigl|\Theta_n(t)v_n(R)\bigr| &\leqslant \bigl|\Theta_n(0)v_n(R)\bigr| \\
&= \left|\frac{T_0\sqrt{k_b c_b\rho_b}}{\lambda_n\|v_n\|^2}\left[R_b\cot(\lambda_n a_b R_b) - \frac{1}{\lambda_n a_b}\right]v_n\right| \\
&\leqslant \frac{\text{const}_2}{\lambda_n^2} \leqslant \frac{\text{const}_3}{n^2}
\end{aligned} \tag{C.4}$$

When deriving condition (C.4), Eq. (19) was used. Estimate of λ_n follows from Eq. (20) for sufficiently large n. Estimate (C.4) means that in the absence of radiation the series in Eq. (10) converges absolutely and uniformly at least in the limit $\varepsilon \to 0$.

Appendix D. The Cesaro method

It can be proven (see [38]) that if the series

$$S(x) = \sum_{n=1}^{\infty} w_n(x) \tag{D.1}$$

converges then

$$S(x) = \lim_{n_{\max}\to\infty}\left[\frac{1}{n_{\max}}\sum_{n=1}^{n_{\max}} S_n(x)\right]$$

where

$$S_n(x) = \sum_{k=1}^{n} w_k(x)$$

The Cesaro method is based on this result, and it allows to rewrite $S(x)$ in the form:

$$\begin{aligned} S(x) &= \lim_{n_{\max}\to\infty}\left[\frac{1}{n_{\max}}\sum_{n=1}^{n_{\max}}\left(\sum_{k=1}^{n} w_k(x)\right)\right] \\ &= \lim_{n_{\max}\to\infty}\left[\frac{1}{n_{\max}}\big(w_1 n_{\max} + w_2(n_{\max}-1) + \cdots \right. \\ &\quad \left. + w_n(n_{\max}-n+1) + \cdots + w_{n_{\max}}\big)\right] \\ &= \lim_{n_{\max}\to\infty}\sum_{n=1}^{n_{\max}} w_n(x)\left(1-\frac{n-1}{n_{\max}}\right) \end{aligned} \tag{D.2}$$

Series (D.2) converges much quicker than the original series (D.1).

Using series (D.2), Eq. (10) has been rearranged for numerical analysis to:

$$\big[T(R,t) - T_{g0}\big]R = \sum_{n=1}^{n_{\max}} w_n(t,R)\left(1-\frac{n-1}{n_{\max}}\right) \tag{D.3}$$

where $n_{\max}$ is the maximal number of terms to be taken into account, $w_n(t, R)$ are the terms in the series in the right-hand side of (10).

References

[1] R.B. Bird, W.E. Stewart, E.N. Lightfoot, Transport Phenomena, John Wiley, New York, 2002.

[2] O.M. Todes, Quasi-stationary regimes of mass and heat transfer between a spherical body and ambient medium, in: V.A. Fedoseev (Ed.), Problems of Evaporation, Combustion and Gas Dynamics of Disperse Systems, Proceedings of the Sixth Conference on Evaporation, Combustion and Gas Dynamics of Disperse Systems, October 1966, Odessa University Publishing House, Odessa, 1968, pp. 151–159 (in Russian).

[3] S.S. Sazhin, V. Goldshtein, M.R. Heikal, A transient formulation of Newton's cooling law for spherical bodies, ASME J. Heat Transfer 123 (2001) 63–64.

[4] Z.-G. Feng, E.E. Michaelides, Unsteady heat transfer from a sphere at small Peclet numbers, ASME J. Fluid Engrg. 118 (1996) 96–102.

[5] F. Cooper, Heat transfer from a sphere to an infinite medium, Int. J. Heat Mass Transfer 20 (1977) 991–993.

[6] M.N. Özişik, Heat Conduction, John Wiley and Sons, New York, 1980.

[7] S.W. Baek, J.H. Park, S.J. Kang, Transient cooling of a two-phase medium of spherical shape when exposed to rarefied cold environment, Int. J. Heat Mass Transfer 44 (2001) 2345–2356.

[8] P. Sadooghi, C. Aghanajafi, Coating effects on transient cooling a hot spherical body, J. Fusion Energy 22 (2004) 59–65.

[9] H. Malissa (Ed.), Analysis of Airborne Particles by Physics Methods, CRC Press, Florida, 1978.

[10] R.M. Harrison, R.E. van Grieken (Eds.), Atmospheric Particles, John Wiley & Sons, Chichester, 1998.

[11] W.H. Walton (Ed.), Inhaled Particles, vols. 1 and 2, Pergamon Press, Oxford, 1977.

[12] W.A. Sirignano, Fluid Dynamics and Transport of Droplets and Sprays, Cambridge University Press, Cambridge, 1999.

[13] J.F. Griffiths, J.A. Bernard, Flame and Combustion, Blackie Academic & Professional, 1995.

[14] P.F. Flynn, R.P. Durrett, G.L. Hunter, A.O. zur Loye, O.C. Akinyemi, J.E. Dec, C.K. Westbrook, Diesel combustion: An integral view combining laser diagnostics, chemical kinetics, and empirical validation, SAE, Paper 1999-01-0509, 1999.

[15] E.M. Sazhina, S.S. Sazhin, M.R. Heikal, V.I. Babushok, R. Johns, A detailed modelling of the spray ignition process in diesel engines, Combust. Sci. Tech. 160 (2000) 317–344.

[16] S.S. Sazhin, G. Feng, M.R. Heikal, I. Goldfarb, V. Goldshtein, G. Kuzmenko, Thermal ignition analysis of a monodisperse spray with radiation, Combust. Flame 124 (2001) 684–701.

[17] S.S. Sazhin, Advanced models of fuel droplet heating and evaporation, Prog. Energy Combust. Sci. 32 (2006) 162–214.

[18] S.S. Sazhin, P.A. Krutitskii, W.A. Abdelghaffar, E.M. Sazhina, S.V. Mikhalovsky, S.T. Meikle, M.R. Heikal, Transient heating of diesel fuel droplets, Int. J. Heat Mass Transfer 47 (2004) 3327–3340.

[19] S.S. Sazhin, W.A. Abdelghaffar, E.M. Sazhina, M.R. Heikal, Models for droplet transient heating: effects on droplet evaporation, ignition, and break-up, Int. J. Thermal Sci. 44 (2005) 610–622.

[20] S.S. Sazhin, W.A. Abdelghaffar, P.A. Krutitskii, E.M. Sazhina, M.R. Heikal, New approaches to numerical modelling of droplet transient heating and evaporation, Int. J. Heat Mass Transfer 48 (2005) 4215–4228.

[21] S.S. Sazhin, T. Kristyadi, W.A. Abdelghaffar, M.R. Heikal, Models for fuel droplet heating and evaporation: comparative analysis, Fuel 85 (2006) 1613–1630.

[22] V. Bykov, I. Goldfarb, V. Gol'dshtein, S. Sazhin, E. Sazhina, System decomposition technique for spray modelling in CFD codes, Comput. Fluids (2006), in press.

[23] H.S. Carslaw, J.C. Jaeger, Conduction of Heat in Solids, Clarendon Press, Oxford, 1986.

[24] E.M. Kartashov, Analytical Methods in the Heat Transfer Theory in Solids, Vysshaya Shkola, Moscow, 2001 (in Russian).

[25] R. Siegel, J.R. Howell, Thermal Radiation Heat Transfer, Hemisphere, Washington, DC, 1992.

[26] A. Tuntomo, C.L. Tien, S.H. Park, Internal distribution of radiant absorption in a spherical particle, ASME J. Heat Transfer 113 (1991) 402–412.

[27] P.L.C. Lage, R.H. Rangel, Single droplet vaporization including thermal radiation absorption, J. Thermophys. Heat Transfer 7 (1993) 502–509.

[28] L.A. Dombrovsky, S.S. Sazhin, Absorption of external thermal radiation in asymmetrically illuminated droplets, J. Quantitative Spectrosc. Radiat. Transfer 87 (2004) 119–135.

[29] L.A. Dombrovsky, Absorption of thermal radiation in large semi-transparent particles at arbitrary illumination of a polydisperse system, Int. J. Heat Mass Transfer 47 (2004) 5511–5522.

[30] L.A. Dombrovsky, S.S. Sazhin, Absorption of thermal radiation in a semi-transparent spherical droplet: a simplified model, Int. J. Heat Fluid Flow 24 (2003) 919–927.

[31] L.A. Dombrovsky, S.S. Sazhin, E.M. Sazhina, G. Feng, M.R. Heikal, M.E.A. Bardsley, S.V. Mikhalovsky, Heating and evaporation of semi-transparent diesel fuel droplets in the presence of thermal radiation, Fuel 80 (2001) 1535–1544.

[32] S.S. Sazhin, W.A. Abdelghaffar, E.M. Sazhina, S.V. Mikhalovsky, S.T. Meikle, C. Bai, Radiative heating of semi-transparent diesel fuel droplets, ASME J. Heat Transfer 126 (2004) 105–109;
S.S. Sazhin, W.A. Abdelghaffar, E.M. Sazhina, S.V. Mikhalovsky, S.T. Meikle, C. Bai, ASME J. Heat Transfer 126 (2004) 490–491, Erratum.

[33] B. Abramzon, S. Sazhin, Droplet vaporization model in the presence of thermal radiation, Int. J. Heat Mass Transfer 48 (2005) 1868–1873.

[34] B. Abramzon, S. Sazhin, Convective vaporization of fuel droplets with thermal radiation absorption, Fuel 85 (2006) 32–46.

[35] C.A. Sleicher, S.W. Churchill, Radiant heating of dispersed particles, Industr. Engrg. Chemistry 48 (1956) 1819–1824.

[36] R. Viscanta, R.L. Merriam, Heat transfer by combined conduction and radiation between concentric spheres separated by radiating medium, ASME J. Heat Transfer 90 (1968) 248–256.

[37] T. Saitoh, K. Yamazaki, R. Viscanta, Effect of thermal radiation on transient combustion of a fuel droplet, J. Thermophys. Heat Transfer 7 (1993) 94–100.

[38] N.K. Berr, Trigonometrical Series, Fizmatgiz, Moscow, 1961 (in Russian).

[39] A.N. Tikhonov, A.A. Samarsky, Equations of Mathematical Physics, Nauka, Moscow, 1972 (in Russian).

[40] V.S. Vladimirov, Equations of Mathematical Physics, Marcel Dekker, New York, 1971.